Interannual variations of stationary planetary wave activity in the northern winter troposphere and stratosphere and their relations to NAM and SST

Wen Chen

Laboratory of Numerical Modeling for Atmospheric Sciences and Geophysical Fluid Dynamics (LASG), Institute of Atmospheric Physics, Chinese Academy of Sciences, Beijing, China

Masaaki Takahashi

Center for Climate System Research, University of Tokyo, Tokyo, Japan

Hans-F. Graf

Max-Planck-Institute for Meteorology, Hamburg, Germany

Received 4 June 2003; revised 26 October 2003; accepted 4 November 2003; published 31 December 2003.

[1] With the National Centers for Environmental Prediction-National Center for Atmospheric Research (NCEP-NCAR) reanalysis data from 1958 to 1998, two teleconnection patterns in the Eliassen-Palm (EP) flux divergence field due to stationary planetary waves with wavenumbers (WNs) 1 to 3 are studied in the Northern Hemisphere winter. Both patterns appear as dipole structures with divergence of EP flux in the north and convergence in the south, or vice versa. One dipole evolves mainly in the stratosphere and is referred to as the stratospheric interannual oscillation (SIO). The other evolves mostly in the troposphere and is referred to as the tropospheric interannual oscillation (TIO). The TIO and the SIO are shown to be associated with anomalous meridional planetary wave propagation in the troposphere and stratosphere, respectively. The upward and poleward refraction of planetary waves into the polar waveguide across the tropopause is closely linked to the TIO. Examination of individual waves indicates that the tropospheric dipole of EP flux divergence comes basically from WN 3, whereas the stratospheric one comes totally from WNs 1 and 2. The reduced refraction of planetary waves into the polar waveguide across the tropopause associated with positive TIO index is dominantly contributed from both WNs 1 and 2. Regression and correlation analyses suggest that the TIO is closely related to the Northern Annular Mode (NAM). Its relation to the sea surface temperature (SST) is consistent with previous studies on the relation of NAM to SST. On the other hand, the SIO is shown to be closely associated with anomalous zonal mean winds in the subtropics of the midstratosphere and has a moderate correlation with an augmented Pacific-North American (PNA) pattern in 500 hPa geopotential height. For the leading EOF of stratospheric $\bar{u}$ variability the SIO accounts for a smaller fraction than the TIO. However, with the teleconnectivity in stratospheric EP flux divergence one can distinguish a stratospheric variation of anomalous north-south planetary wave propagation from the total amount of wave activity entering the stratosphere, which may help us to understand the variability of transport circulation in the stratosphere. Significant correlation of SIO with tropical SST reveals that tropical SST is leading the SIO by up to around 9 months, which suggests a strong impact of El Niño/Southern Oscillation (ENSO) on the SIO. Planetary waves tend to be bent poleward in the midstratosphere when there is a warm event. The situation tends to be reverse during a cold event. *INDEX TERMS:* 3309 Meteorology and Atmospheric Dynamics: Climatology (1620); 3319 Meteorology and Atmospheric Dynamics: General circulation; 3384 Meteorology and Atmospheric Dynamics: Waves and tides; 3362 Meteorology and Atmospheric Dynamics: Stratosphere/troposphere interactions; *KEYWORDS:* planetary waves, interannual variation, SST

Citation: Chen, W., M. Takahashi, H.-F. Graf, Interannual variations of stationary planetary wave activity in the northern winter troposphere and stratosphere and their relations to NAM and SST, *J. Geophys. Res.*, *108*(D24), 4797, doi:10.1029/2003JD003834, 2003.

0148-0227/03/2003JD003834

1. Introduction

[2] In the Northern Hemisphere (NH) winter, the stratospheric and tropospheric circulations are dynamically linked through the interaction of mean flow with upward propagating planetary-scale waves [*Matsuno*, 1970]. There is strong evidence that much of the planetary wave activity observed in the winter stratosphere is excited in the troposphere [e.g., *Randel*, 1987, and references therein]. The most obvious tropospheric sources of planetary waves are associated with geographical asymmetries such as topography and patterns of diabatic heating arising from the distribution of land and sea [*Andrews et al.*, 1987]. Stationary planetary waves in the winter stratosphere are primarily due to these geographical asymmetries. In the NH, where geographical asymmetries are large, the wintertime stratosphere is dominated by stationary planetary waves [*Scinocca and Haynes*, 1998]. On the other hand, observational data and experiments with atmospheric general circulation models (AGCMs) indicate a slow downward propagation of zonal wind anomalies from the stratosphere into the troposphere through the interaction of upward propagating waves with the mean flow [*Baldwin and Dunkerton*, 1999; *Kuroda and Kodera*, 1999]. It is well known that there is large interannual variability in the northern winter stratospheric zonal wind [*Labitzke*, 1982; *Kodera*, 1995], and much effort has gone into finding possible stratospheric and tropospheric causes for this variability. Part of the NH variability may be linked to the quasi-biennial oscillation (QBO) in the equatorial lower stratosphere, which appears to modulate the propagation of extratropical planetary waves and hence their forcing of the zonal-mean flow [*Holton and Tan*, 1982; *Niwano and Takahashi*, 1998; *Chen and Huang*, 1999]. In addition, variations of the winter mean stratospheric zonal winds are well correlated with the strength of a pattern in the troposphere very similar to the North Atlantic Oscillation (NAO) [*Baldwin et al.*, 1994; *Perlwitz and Graf*, 1995; *Ambaum et al.*, 2001]. However, with a stratospheric model, *Kinnersley* [1998] suggested that planetary wave variability in the lower stratosphere was the direct cause of much of the interannual variability of stratospheric zonal wind during the NH winter. Therefore, the precise relations between stratospheric and tropospheric planetary waves and the associated variations of zonal wind are not well understood yet.

[3] Recent observations indicate that month-to-month and winter-to-winter variations in the NH are dominated by a zonally symmetric, meridional seesaw of atmospheric mass across the midlatitudes [*Thompson and Wallace*, 1998; *Baldwin and Dunkerton*, 1999]. This mode was referred to as the Northern Annular Mode (NAM). The NAM also corresponds to a north-south seesaw of zonal-mean zonal wind ($\bar{u}$) between around 35°N and 55°N [*Thompson and Wallace*, 2000]. NH $\bar{u}$ fluctuations are generally accompanied by large-amplitude stationary waves [*Branstator*, 1984; *Ting et al.*, 1996]. The relationship between the zonal-mean and eddy flow anomalies has been suggested to be due to mutual adjustment by *DeWeaver and Nigam* [2000]. *Limpasuvan and Hartmann* [1999, 2000] showed that variations of the NAM are forced by eddy fluxes mainly of stationary waves in the free troposphere of the NH. The changes in the strength of the stratospheric polar vortex during winter were further linked to the changes in tropospheric NAM by the planetary wave propagation characteristics. The NAM can be simulated in an AGCM with climatological sea surface temperature (SST) [e.g., *Yamazaki and Shinya*, 1999; *Limpasuvan and Hartmann*, 2000]. It was then suggested that the NAM is basically an internal mode of the atmosphere which may occur in the absence of any external forcing. However, the low-frequency behavior of NAM could be influenced by external forcings such as SSTs [*Rodwell et al.*, 1999; *Watanabe and Kimoto*, 2000], snow cover [*Kodera and Koide*, 1997], and anthropogenic emissions reducing stratospheric ozone or increasing the greenhouse gas concentration in the Earth's atmosphere [*Graf et al.*, 1998; *Shindell et al.*, 1999]. Especially the influence of SSTs is still a matter of some debate. With AGCM studies Rodwell et al. argued that a positive feedback between a tripolar North Atlantic SST pattern and the NAO was responsible for this oceanic influence, while *Latif et al.* [2000] and *Hoerling et al.* [2001] suggested that the bulk of the oceanic influence might come from the tropical belt. These controversial results emphasize that the response of AGCMs to prescribed SST anomalies is strongly model-dependent [*Robinson*, 2000]. Accordingly, more observational studies are needed to determine the influence of SST on the stationary waves, which provides the important forcing to the zonal-mean flow.

[4] In this paper we will focus on the stationary planetary wave activity both in the troposphere and in the stratosphere. *Fusco and Salby* [1999] and *Salby et al.* [2000] found that on interannual timescales stratospheric ozone and temperature in the Arctic polar region in winter is regulated by the upward Eliassen-Palm (EP) flux across the tropopause, and that the two have a strong correlation. Based on the AGCM simulations under increased greenhouse gas forcing, *Rind et al.* [1998] and *Shindell et al.* [1998, 1999] speculated that the planetary wave activity from the troposphere to the stratosphere might have declined. An understanding of interannual variations of planetary wave activity may thus be necessary to properly identify anthropogenic changes.

[5] Recently work of *Chen et al.* [2002] had found two independent oscillations for planetary wave forcing in the troposphere and stratosphere, respectively. Their interannual variations of planetary waves propagation and the associated changes in atmospheric circulation are studied to more extent here, and further relationships to SST are also examined. The data sources and methods are introduced in section 2, followed in section 3 by a description of the climatology and teleconnection patterns for planetary wave activity. In section 4 and 5, we discuss the interannual variations of planetary wave activity in the troposphere and stratosphere, respectively. Their possible origins from the atmosphere or the ocean are further analyzed. Finally, in section 6 we conclude with a brief discussion of the results of the present study.

2. Data and Methods

[6] This study is based on the monthly mean pressure level data of 41 years (1958–1998) from the National Centers for Environmental Prediction-National Center for

Atmospheric Research (NCEP-NCAR) reanalysis [*Kalnay et al.*, 1996]. The reanalysis data set is known to be probably unreliable at stratospheric levels before 1958 due to the lack of sufficient observational data in the upper atmosphere [*Kistler et al.*, 2001]. The data set has a 2.5° × 2.5° horizontal resolution and extends from 1000 to 10 hPa with 17 vertical pressure levels. We also employ the reconstructed monthly SST data obtained from NCAR's Data Support Section (http://dss.ucar.edu/catalogs/free.html). These data are available from January 1950 to the present, with a grid of 2° by 2° [*Reynolds and Smith*, 1995]. The seasonal means are constructed by averaging December, January and February (DJF) resulting in 40 winter fields.

[7] As a diagnostic tool, the EP flux is used, which is a measure of the wave activity propagation [*Andrews et al.*, 1987]. The quasi-geostrophic version of EP flux in spherical geometry is employed in calculating its divergence due to planetary waves [*Edmon et al.*, 1980], which indicates the eddy forcing of the zonal mean flow. The components of EP flux ($\vec{F}$) and its divergence (D_F) are

$$F_y = -\rho a \cos\varphi \overline{u'v'}, \quad F_z = \rho a \cos\varphi \frac{Rf}{HN^2}\overline{v'T'}, \quad D_F = \frac{\nabla \cdot \vec{F}}{\rho a \cos\varphi},$$

where ρ is air density, a is the radius of the earth, φ is the latitude, R is the gas constant, f is the Coriolis parameter, H is a constant-scale height (7 km), N is the buoyancy frequency, u and v are zonal and meridional wind, T is temperature, primes denote zonal deviation, and overbars denote zonal average. Here N is calculated from the temperature data. By expanding the seasonal mean (DJF) geopotential height field into their zonal Fourier harmonics, the sum of zonal wavenumbers (WNs) 1 through 3 is used to represent stationary planetary wave activity for each individual winter. Then they are used to calculate the quasi-geostrophic EP flux and its divergence. It should be noted that we didn't find the overestimation of the geostrophic momentum flux divergence suggested by *Robinson* [1986]. The results of quasi-geostrophic EP flux divergence are quite similar to those directly using winds.

[8] Correlation and regression studies are adopted throughout this paper. If the individual 40 winters of data are independent of each other, the correlation coefficients corresponding to the 95% and 99% significance levels are 0.31 and 0.40, respectively. Since the effective number of degrees of freedom (EDOF) may not be the same as the number of data that enter into the calculation, we consequently used the EDOF according to *Davis* [1976] to check the statistical significance.

3. Climatology and Teleconnection Patterns for Planetary Wave Activity

[9] Before analyzing the variations of planetary wave activity, it is helpful to look at its climatology. Figure 1a shows the average EP flux cross sections of zonal waves 1 to 3 and its divergence pattern for winters (DJF) from 1958–1998 in the NH. It is clear in Figure 1a that planetary waves propagate upward from the lower boundary at midlatitudes, and split into two branches in the upper troposphere with one branch going equatorward and the other propagating into the stratosphere. In most of the extratropical troposphere the EP flux is convergent, which means an easterly zonal force on the atmosphere exerted by planetary waves. In the stratosphere planetary waves turn toward the tropics after penetration into the middle stratosphere, and for the distribution of EP flux divergence there is a dipole pattern with convergence in the midlatitudes and divergence in the high latitudes. The diagram compares well to the theoretical and simulated results of planetary wave propagation [*Matsuno*, 1970; *Chen and Huang*, 1999] and to the observations [*Dunkerton and Baldwin*, 1991]. Detailed analysis of individual stationary waves indicates that for WNs 1 (Figure 1b) and 2 (Figure 1c) the waves can propagate into the stratosphere and contribute to the dipole pattern of EP flux divergence as shown in Figure 1a. However, for WN 3 the wave is confined mainly to the troposphere and does not contribute to the wave forcing in the stratosphere (Figure 1d).

[10] In order to identify the recurrent spatial patterns which may be indicative of standing oscillations in the planetary waves, *Chen et al.* [2002] calculated the teleconnectivity in the EP flux divergence field as *Wallace and Gutzler* [1981] but in the latitude pressure domain. With teleconnectivity they avoid the problems with the EOF analysis, which not necessarily come up with physically based structures and then need justification [*Deser*, 2000; *Ambaum et al.*, 2001]. By examination of the one-point correlation maps they found two teleconnection patterns for planetary wave forcing, with one in the stratosphere and the other in the troposphere. The winter mean pattern indices were defined based on the EP flux divergence anomalies at specified grid points corresponding to centers of action. Chen et al. defined the stratospheric pattern index as the difference of EP flux divergence between 75°N and 57.5°N at 30 hPa, and the tropospheric pattern index as that between 50°N at 500 hPa and 40°N at 300 hPa. It has also been found that the results in the paper are not sensitive to subtle changes in the centers of action of the two indices. Here, a positive pattern index is indicative of anomalously divergence of EP flux in the north and convergence in the south; a negative pattern index indicates anomalies of the opposite sign.

[11] Figures 2a and 3a present the time series of the two indices from 1959 to 1998 together with their linear trends. The convention here is that the "1959" northern winter is actually 1958/1959 and so on. The tropospheric index (Figure 3a) has an evident linear trend toward its positive polarity with statistical significance above 99%, whereas the stratospheric one (Figure 2a) is slightly increasing over recent decades, but not statistically significant. The correlation coefficients of the EP flux divergences at each grid point with the two indices are shown in Figures 2b and 3b, respectively. For stratospheric index (Figure 2b), large correlation values appear mostly in the stratosphere with only marginal correlations in the troposphere. In the reference points A (30 hPa, 75°N) and B (30 hPa, 57.5°N) the correlation values are 0.99 and −0.82, respectively. For the tropospheric index (Figure 3b), large correlation values are mainly in the troposphere with extension to the stratosphere. In the reference points C (500 hPa, 50°N) and D (300 hPa, 40°N) the correlation values are 0.96 and −0.85, respec-

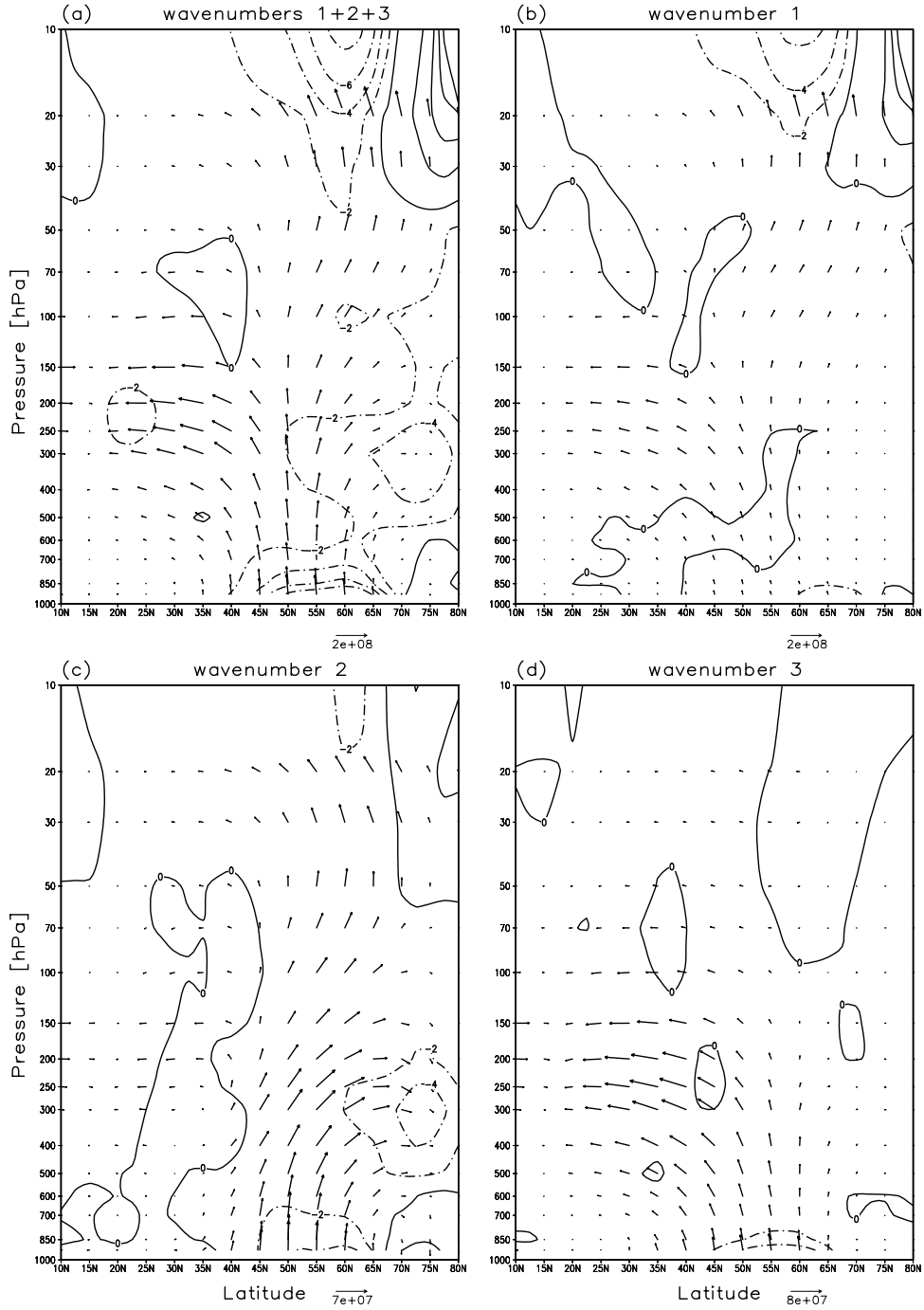

Figure 1. EP flux cross sections (vectors) and its divergence (contours) averaged for 40 winters from 1958 to 1998. (a) For the sum of zonal wavenumbers 1 to 3; (b) for wavenumber 1; (c) for wavenumber 2; and (d) for wavenumber 3. EP fluxes are scaled by the inverse of the air density. Divergence contour interval is 2 $ms^{-1}day^{-1}$, with negative values dashed.

tively. Both the correlation patterns in Figures 2b and 3b are very similar to the one-point correlation maps based on the corresponding reference points [see *Chen et al.*, 2002, Figure 2]. The correlation between the two time series shown in Figures 2a and 3a is 0.2. If both indices are detrended by subtraction of their linear trends, the correlation of them is only 0.17. These suggest that the stratospheric oscillation is different from the tropospheric one on the interannual timescale. In order to make them easy to refer to, we shall call those two time variations in Figures 2a and 3a the stratospheric interannual oscillation (SIO) and the tropospheric interannual oscillation (TIO) for planetary wave forcing, respectively.

[12] In the following, we will discuss the variations of planetary wave activity on the interannual timescale. Accordingly, the indices are detrended by subtraction of their linear trends. All other data are also detrended by subtraction of local linear trends. The linear correlation and

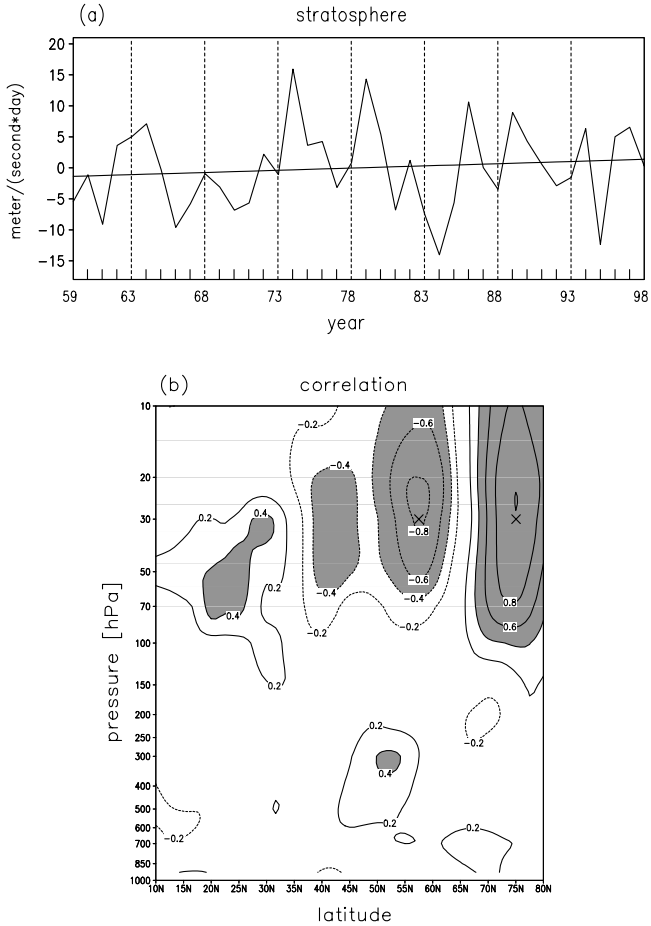

Figure 2. (a) Winter mean (DJF) time series (1957/58 ~ 1997/98) of the stratospheric teleconnection pattern index together with the linear trend function. (b) Correlation coefficients between the stratospheric teleconnection pattern index and the EP flux divergences at each grid point for 40 winters. The two reference points A (30 hPa, 75°N) and B (30 hPa, 57.5°N) are marked with "crosses." The contour interval is 0.2 and the zero contour line has been suppressed. The areas are shaded for absolute values of correlation coefficients $\geq$0.4.

regression analyses are carried out in order to assess atmospheric circulation and SST anomalies associated with the interannual variations of planetary wave activity. As a matter of fact, it has been found that the conclusions presented in the paper are not changed if the data were not detrended.

4. Planetary Wave Activity Associated With the TIO and Its Relations to NAM and SST

4.1. Planetary Wave Activity Associated With the TIO

[13] With the detrended TIO index and EP flux divergence field, we calculated the correlation coefficients at each grid point. The results are nearly the same as in Figure 3b (figure not shown). The correlation values are 0.95 and −0.83 in the reference points C and D, respectively. Figure 4 shows the regression map of EP flux cross sections and its divergence on the TIO index for the sum of zonal WNs 1 to 3 and each zonal WN component. For the sum of zonal WNs 1 to 3 (Figure 4a), a dipole of anomalous EP flux divergence appears in the midlatitudes of the troposphere, with the centers of action in C and D exactly. This dipole is associated with anomalous meridional propagation of planetary waves in the troposphere. In addition, the upward wave propagation tends to be reduced much around 35°–55°N and enhanced a little around 60°–70°N in the lower troposphere. There is also anomalous EP flux divergence along the polar waveguide high up into the stratosphere associated with the positive TIO index. The anomalous EP flux cross sections suggest that the upward and poleward wave refraction into the polar waveguide in the lower stratosphere is reduced (mainly due to WN 1, see Figure 4b), and the waves tend to be bent equatorward in the stratosphere (mainly due to WN 2, see Figure 4c) for a positive TIO index. Combination of Figures 3b and 4a suggests that the upward and poleward refraction of planetary waves into the polar waveguide across the tropopause is closely linked to the meridional propagation of planetary waves in the troposphere. During the positive TIO phase, the equatorward propagation of planetary waves in the troposphere tends to be enhanced. At the same time the

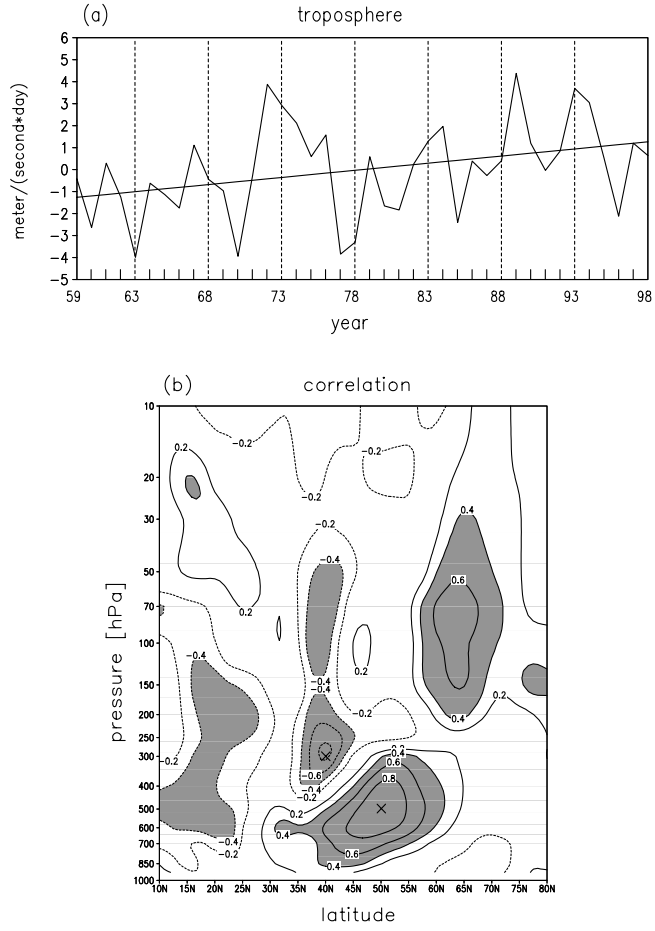

Figure 3. The same as in Figure 2, but for tropospheric teleconnection pattern index. The two reference points C (500 hPa, 50°N) and D (300 hPa, 40°N) are marked with "crosses" in (b).

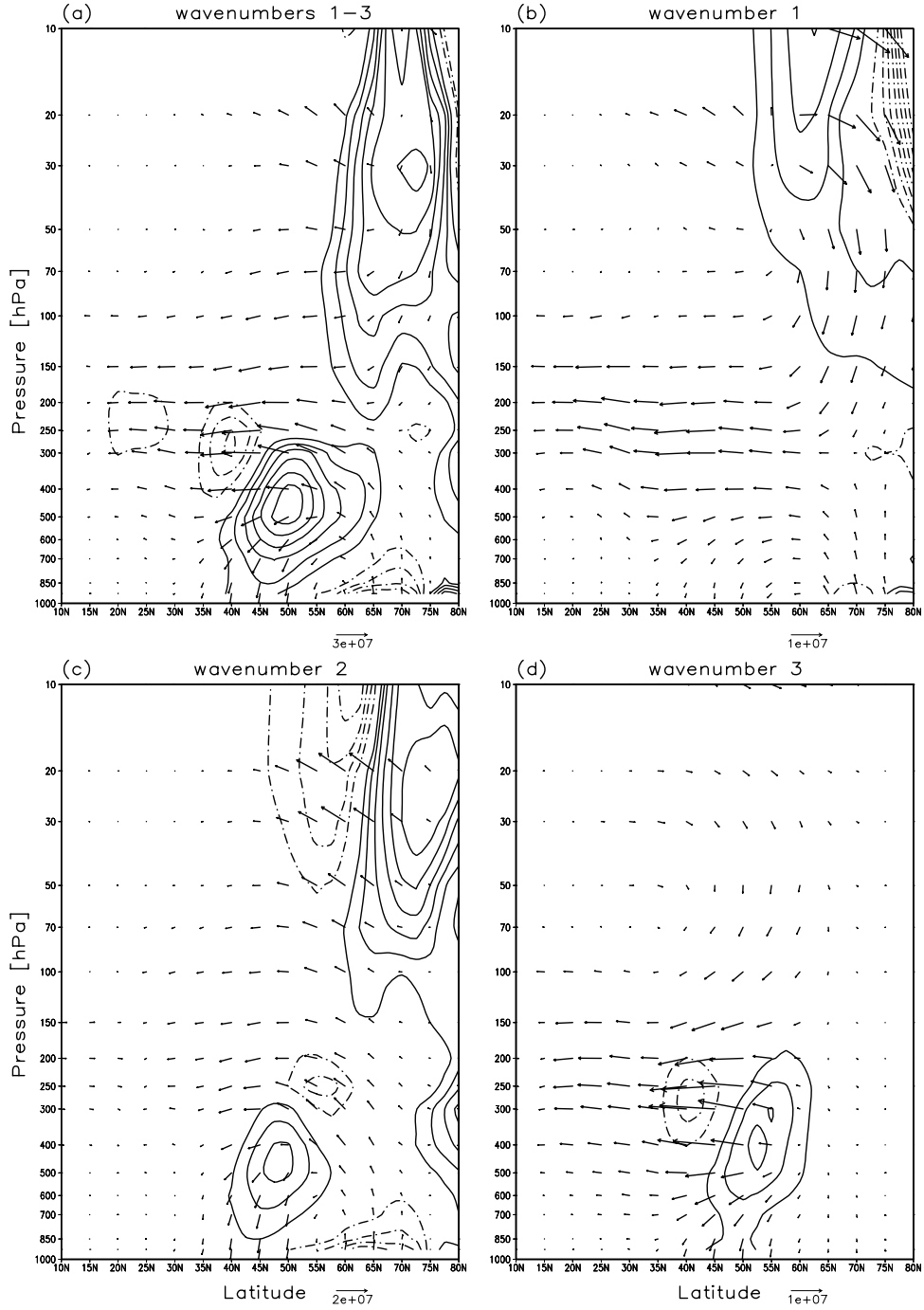

Figure 4. EP flux cross sections of planetary waves (vectors) and its divergence (contours) regressed on the normalized TIO index based on winter data from 1959 to 1998. (a) For the sum of zonal wavenumbers 1 to 3; (b) for wavenumber 1; (c) for wavenumber 2; and (d) for wavenumber 3. EP fluxes are scaled by the inverse of the air density. Unit for EP flux divergence is $ms^{-1}day^{-1}$. Contour interval is 0.2. The zero contour line has been suppressed and the dashed lines indicate negative values. The data are detrended by subtraction of local linear trends.

upward and poleward propagation of planetary waves into the polar waveguide in the lower stratosphere tends to be reduced. Figure 3 indicates a significant trend of TIO index towards its positive polarity. This means a reduced upward planetary wave propagation into the stratosphere in recent decades and convinces the results of *Rind et al.* [1998] and *Shindell et al.* [1998, 1999].

[14] Examination of each WN component indicates that the dipole in the troposphere as shown in Figure 4a comes basically from WN 3 (Figure 4d). The wave of WN 3 tends to be bent equatorward in the midlatitudes from midtroposphere to lower stratosphere. For WN 2, it is evident that the upward wave propagation tends to be reduced much around 35°–55°N and enhanced a little around 60°–70°N in the

lower troposphere (Figure 4c). This induces anomalous divergence of EP flux in the midlatitudes of the troposphere, and suggests that WN 2 is also important in contributing to the positive anomaly in the troposphere in Figure 4a. The wave of WN 1 (Figure 4b) has nearly no contribution to the tropospheric dipole pattern. The anomalous EP flux divergence along the polar waveguide in the stratosphere, as shown in Figure 4a, comes totally from WNs 1 and 2 (Figures 4b and 4c). Especially in the area centered at point (65°N, 100 hPa) both, WNs 1 and 2, have similar contribution, where it shows a large positive correlation to the TIO index. However, the anomalous wave propagations associated with the TIO are different for WNs 1 and 2. For WN 1, it is evident that the upward wave propagation tends to be reduced poleward of 60°N in the stratosphere (Figure 4b). The wave tends to be further bent equatorward in the lower stratosphere and upper troposphere. For WN 2, the wave tends to be bent equatorward in the stratosphere including upper troposphere. Both propagations of WNs 1 and 2 are associated with the anomalous divergence of EP flux in the lower stratosphere. However, in the midstratosphere anomalous wave propagations for WNs 1 and 2 are nearly reverse and tend to induce opposite anomalies in EP flux divergence (Figures 4b and 4c). Probably there are strong wave-wave interactions instead of wave-zonal mean flow interactions over that region. Our results suggest that the wave activity in the midstratosphere is not closely associated with the TIO.

4.2. Relationship to the NAM

[15] Figure 5a shows the regression (contours)/correlation (shading) map of $\bar{u}$ upon the TIO index. The regression pattern is an equivalent barotropic dipole extending from the lower boundary to the upper stratosphere with reduced westerlies around 35°N and enhanced westerlies around 55°N for positive TIO. The high-latitude centers of the winds tilt poleward with height from 55°N in the lower troposphere to ~65°N in the stratosphere. This pattern of $\bar{u}$ anomalies strongly resembles the leading $\bar{u}$ EOF as presented by a number of studies [e.g., *DeWeaver and Nigam*, 2000; *Thompson and Wallace*, 2000]. Figure 5b presents the result of regression (contours)/correlation (shading) map of the NH (poleward of 20°N) 500 hPa geopotential height upon the TIO index. The spatial structure of geopotential height anomalies regressed upon the TIO index is predominantly zonally symmetric, and closely resembles the regression pattern for 500 hPa geopotential height based upon the leading principal component of wintertime (November to April) monthly mean sea-level pressure (SLP) anomalies (the NAM index) [see *Thompson and Wallace*, 1998, Figure 1]. The north-south fluctuation appears with low heights over the Arctic region and high heights mainly over the midlatitude oceanic sectors corresponding to the positive TIO index. Accordingly, we constructed the winter NAM index from 1959 to 1998 by averaging DJF based on monthly index values (data from D. Thompson's Annular Modes website http://horizon.atmos.colostate.edu/ao/Data/index.html). Detailed information of the NAM index can be found in *Thompson and Wallace* [2000]. The winter NAM index has exhibited a large and significant trend toward the high index polarity over the past few decades [*Thompson et al.*, 2000]. The temporal correlation between the detrended NAM index and the TIO index is 0.69, which is significant to 99% confidence. Therefore, one can conclude that the TIO is closely associated with the NAM.

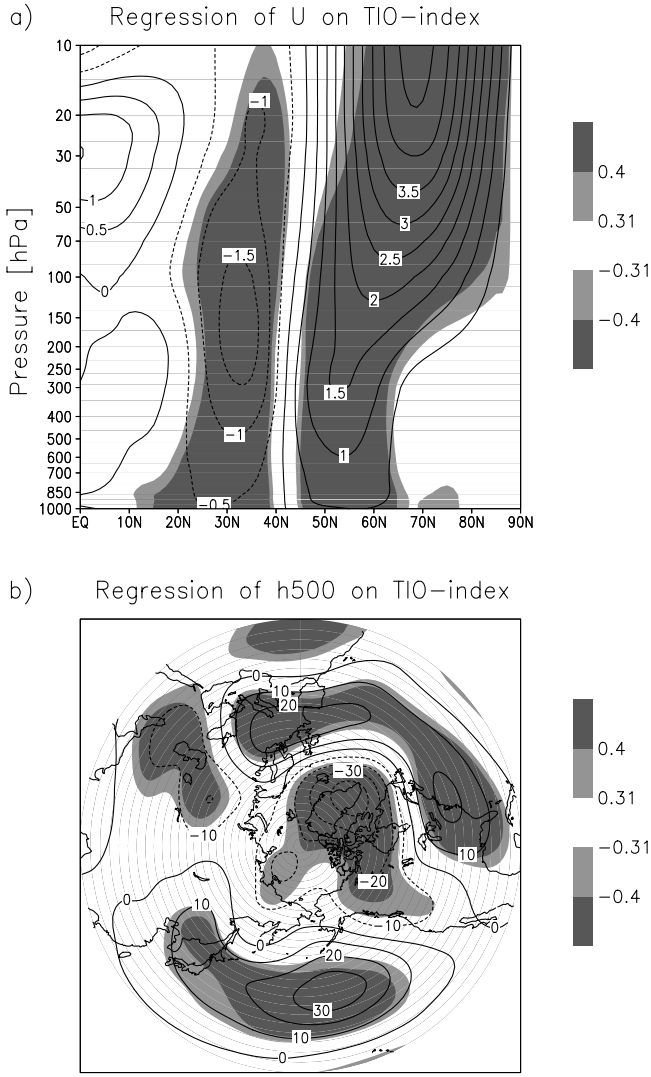

Figure 5. Regression (contours)/correlation (shading) maps for the zonal-mean zonal winds (a) and the geopotential heights at 500 hPa (b) on the normalized TIO index based on winter data from 1959 to 1998. The shading indicates that the correlation is significant above the 95%- (light) and the 99%-level (dark), respectively. The data are detrended by subtraction of local linear trends too. Contour intervals are 0.5 ms^{-1} in (a) and 10 m in (b).

4.3. Relationship to SST

[16] Figure 6 illustrates the regression pattern of SST upon the TIO index based on the winter data from 1958 to 1998. It is evident that the spatial structure of SST anomalies exhibits a sandwich pattern in the North Pacific and a tripole pattern in the North Atlantic. Similar patterns are derived and described in numerous previous studies [e.g., *Marshall et al.*, 2001, and references therein]. Moreover, the map of simultaneous correlations between the TIO index and SST for the period 1958 to 1998 shows very similar

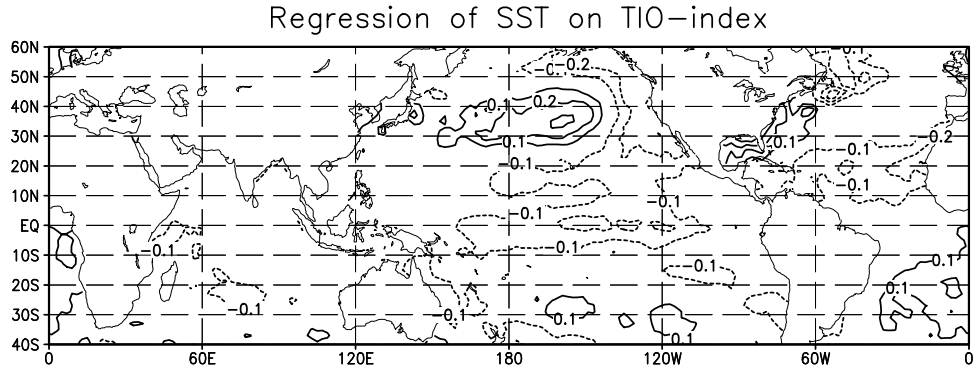

Figure 6. SST anomalies regressed on the normalized TIO index based on winter data from 1959 to 1998. The data are detrended by subtraction of local linear trends too. Contour interval is 0.1°C and the zero contour line has been suppressed.

pattern as in Figure 6 in both North Pacific and North Atlantic (see Figure 7b). In fact, the centers of action in Figure 6, which we mentioned above, are significantly correlated with the TIO index above the 99% level except the negative anomalies between 40° and 60°N in North Atlantic. Although there are negative SST anomalies in the tropical central Pacific in Figure 6, they are not significantly correlated with the TIO index (Figure 7b).

[17] *Frankignoul and Hasselmann* [1977] have pointed out that unlagged correlation between SST and atmospheric anomalies were primarily reflecting the atmospheric forcing to the ocean, so that the oceanic influence on the atmosphere can only be established by studying their covariability when the ocean is leading. *Czaja and Frankignoul* [2002] further suggest that the covariability at 1-month lead is still affected by the atmosphere forcing to the ocean, since the large-scale patterns like the NAO have a significant intrinsic persistence. Figure 7a presents the correlation coefficients between the TIO index and the preceding autumn SST anomalies averaged for September, October and November (SON). Evidently the significant correlation pattern of Figure 7b cannot be traced back to the preceding season, except with some large correlations over the subtropical North Atlantic. However, this significant correlation pattern may persist until the following spring (March, April and May (MAM)) mean especially in the North Atlantic (Figure 7c). These results suggest a dominant influence of the atmospheric circulation on the SST, which are in agreement with previous studies [*Marshall et al.*, 2001].

5. Planetary Wave Activity Associated With the SIO and Its Relation to ENSO

5.1. Planetary Wave Activity Associated With the SIO

[18] Similar to the studies in Section 4.1, we calculated the correlations between the SIO index and EP flux divergence at each grid point with the detrended data by subtraction of their linear trends. The result shows a similar pattern as in Figure 2b (figure not shown). The correlation values are 0.99 at the grid point A and −0.83 at the grid point B. These suggest that the SIO is an important interannual variability in the midstratosphere. Figure 8 presents the regression map of EP flux cross sections and its divergence on the SIO index for the sum of zonal WNs 1 to 3 and each zonal WN component. For the sum of zonal WNs 1 to 3, a north-south dipole pattern of anomalous EP flux divergence evolves in the high latitudes of midstratosphere (Figure 8a). This north-south dipole is associated with anomalous meridional propagation of planetary waves. The planetary waves tend to be bent equatorward and induce anomalous divergence in the north and convergence in the south when SIO is positive. The maximum regression coefficients appear in the highest level of 10 hPa, which suggest a stronger signal in higher altitude. Since it reaches the top boundary of the NCEP-NCAR data, further work is needed with the data of more levels in the upper stratosphere.

[19] The examination on each WN component indicates that the dipole in Figure 8a comes totally from WNs 1 and 2 (Figures 8b and 8c). There is no contribution from WN 3 (Figure 8d), which is consistent with the climatology (see Figure 1) that the wave of WN 3 generally cannot propagate into the midstratosphere. Both waves for WNs 1 and 2 tend to be bent equatorward in the midstratosphere at positive SIO, but there is a difference in the propagation between WNs 1 and 2. The upward wave propagation tends to be reduced around 50°–65°N for WN 1 (Figure 8b) and enhanced around 50°–70°N for WN 2 (Figure 8c) in the midstratosphere. In the lower troposphere, it can be discerned that the upward wave propagation tends to be reduced for WN 2 (Figure 8c) and enhanced for WN 3 (Figure 8d) both around 50°–65°N. However, this wave activity in the troposphere has nearly no effect on zonal mean flow and is not closely associated with the SIO.

5.2. Relationship to the Atmospheric Circulation

[20] Figure 9a shows the regression (contours)/correlation (shading) map of $\bar{u}$ upon the SIO index. With respect to the SIO, the spatial pattern of anomalous $\bar{u}$ has a north-south dipole structure in the midstratosphere. The correlations between the SIO index and $\bar{u}$ anomalies are only modest (Figure 9a). The correlation coefficients in the subtropics of the midstratosphere are significant at the 99% level. However, in the midlatitudes of the midstratosphere the correlation coefficients do not reach the 95% significance level when EDOFs are considered. Thus, a positive SIO index state corresponds to a significant reduction of $\bar{u}$ in the subtropics of the midstratosphere. In addition, there are

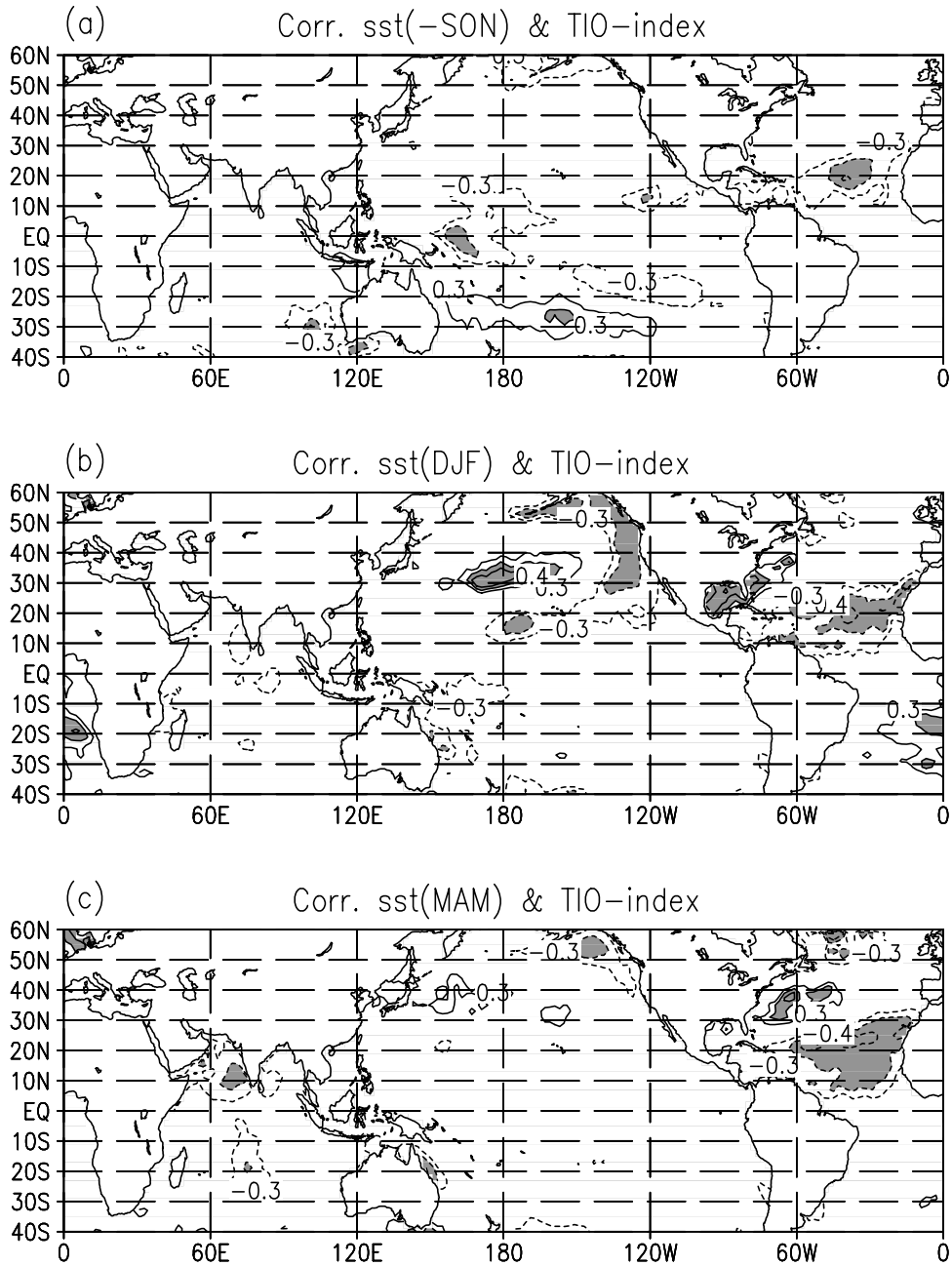

Figure 7. Correlation coefficient between the TIO index and SST at each grid point calculated in (a) the preceding autumn (SON) means, (b) the winter (DJF) means and (c) the following spring (MAM) means for 1958–1998. The contour interval is 0.1, beginning at ±0.3. The areas are shaded for absolute values of correlation coefficients $\geq$0.4.

westerly anomalies in the tropical lower stratosphere for positive SIO, so the signals in Figure 9a appear to be consistent with the result of *Holton and Tan* [1982], who showed that the polar vortex was considerably stronger during the west phase of the equatorial QBO. Therefore, the results here suggest that the QBO may act to modulate the SIO.

[21] In order to know the relation between the SIO and the stratospheric $\bar{u}$ variability, we performed EOF analysis on the seasonal mean $\bar{u}$ anomalies from 100 hPa to 10 hPa. The leading EOF (not shown) indicates a stratospheric variability in $\bar{u}$ along ~65°N and accounts for 47% of the variance. The correlation between the SIO index and the time series for $\bar{u}$ EOF1 is 0.36, while it is 0.55 between the TIO index and the time series for $\bar{u}$ EOF1. The standard deviation of NH winter $\bar{u}$ for the period 1959–1998 and those which is linearly related to the SIO index and the TIO index (Figure 10) indicate that the TIO accounts for a substantially larger fraction of the variance (~55%) of NH stratospheric $\bar{u}$ in the high latitudes than the SIO (~30%), whereas it is opposite in the low latitudes. Therefore, the leading EOF of

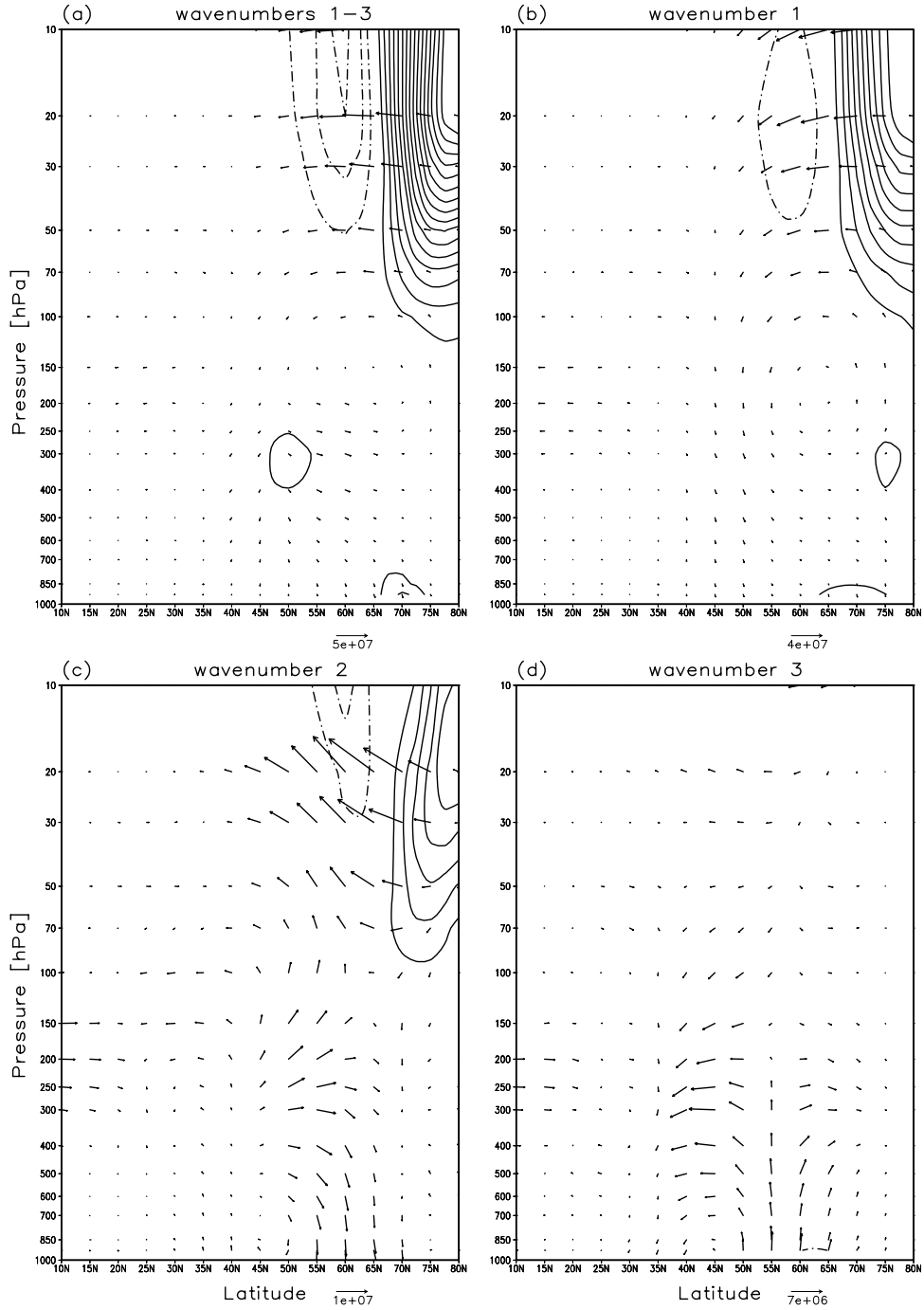

Figure 8. The same as in Figure 4, but on the normalized SIO index. Contour interval is 0.5.

stratospheric $\bar{u}$ variability reflects mainly the variations in the total amount of wave activity entering the stratosphere, not the teleconnectivity in stratospheric EP flux divergence. However, assume the amount of wave activity entering the stratosphere is constant, there is still a variability of anomalous north-south wave activity propagation, which can be sorted out with the teleconnectivity in stratospheric EP flux divergence. Since stationary planetary waves are the dominant wave structure in the stratosphere, this teleconnectivity in stratospheric EP flux divergence may be important to the stratospheric transport circulation.

[22] In the projection of the NH (poleward of 20°N) 500 hPa geopotential height upon the SIO index, the well known PNA wave train appears in combination with another wave train over the Atlantic and Eurasian sectors (Figure 9b). This regression pattern perfectly coincides with the augmented PNA pattern defined by *Wallace and Thompson* [2002] when they regressed the 500 hPa height field on standardized time series corresponding to the second EOF of the NH monthly mean SLP. In the previous section, we have shown that the TIO is closely associated with the NAM, which is the leading EOF of NH SLP field. Here, the SIO is linked to the augmented

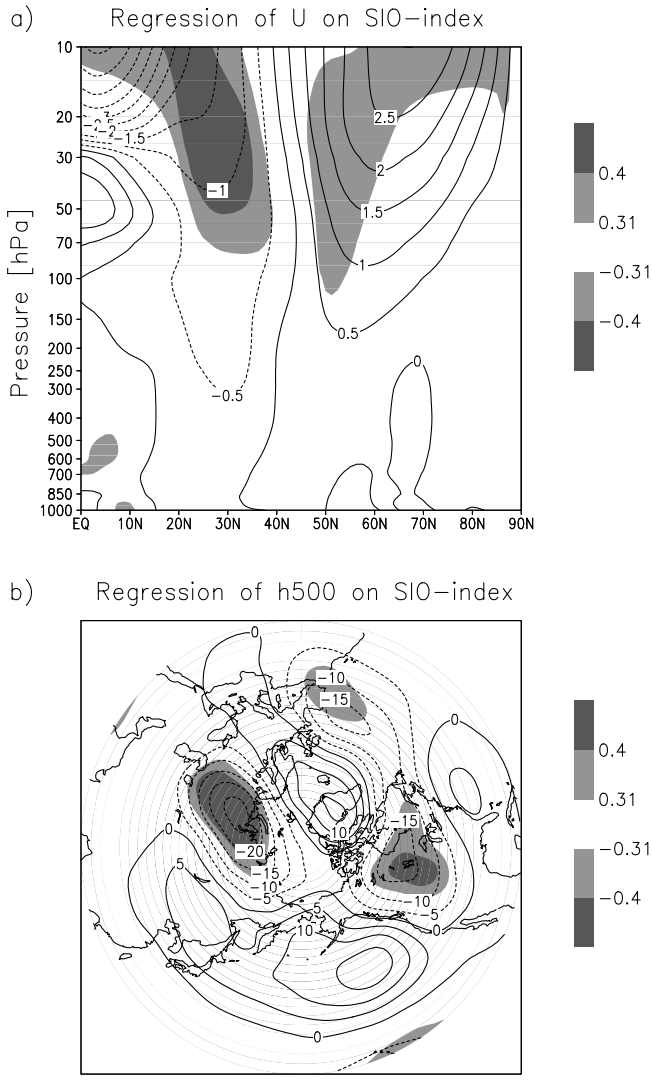

Figure 9. The same as in Figure 5, but on the normalized SIO index. Contour intervals are 0.5 ms^{-1} in (a) and 5 m in (b).

PNA, the second EOF of NH SLP field. However, the correlations between the 500 hPa height anomalies and the SIO index are moderate, with absolute values over 0.4 only in two centers of action over Siberia and North America, respectively. The result here again suggests that the stratospheric planetary wave activity associated with the SIO may not be strongly forced by extratropical circulation anomalies in the troposphere.

5.3. Relationship to El Niño/Southern Oscillation

[23] Figure 11 gives the regression map of SST upon the SIO index based on the winter data from 1958 to 1998. A remarkable signal in SST field exhibits over the central and eastern tropical Pacific, which also has a significant negative correlation with the SIO index (Figure 12b). This spatial structure can be easily identified to be in association with the El Niño/Southern Oscillation (ENSO). When there is a warm event, planetary waves tend to be bent poleward in the midstratosphere. The situation tends to be reverse for a cold event. As we discussed in section 5.2, the QBO is probably modulating the effect; however, the separation of ENSO effects from QBO influences is problematic [*Hamilton*, 1993]. The use of satellite data since 1979 in the NCEP reanalysis leads to spurious changes in the tropics, which has a strong effect on the variability analyses [*Pawson and Fiorino*, 1999], so further discussion of the relationship among ENSO, QBO and SIO will be made in a future work. Combination of the correlations between SIO with SST (Figure 12b) and with $\bar{u}$ (Figure 9a) suggests a possible connection between subtropical midstratospheric zonal winds with tropical eastern Pacific SST; i.e., in a warm ENSO event these winds have stronger westerly anomalies between 20°N and 35°N. It is confirmed by the regression of $\bar{u}$ upon the Niño3 index for the DJF season (Figure 13). This pattern of $\bar{u}$ anomalies in the stratosphere is very similar to that associated with the SIO. The difference is that there are also significant $\bar{u}$ anomalies in the subtropics of the troposphere and the lower stratosphere. A connection to the polar vortex

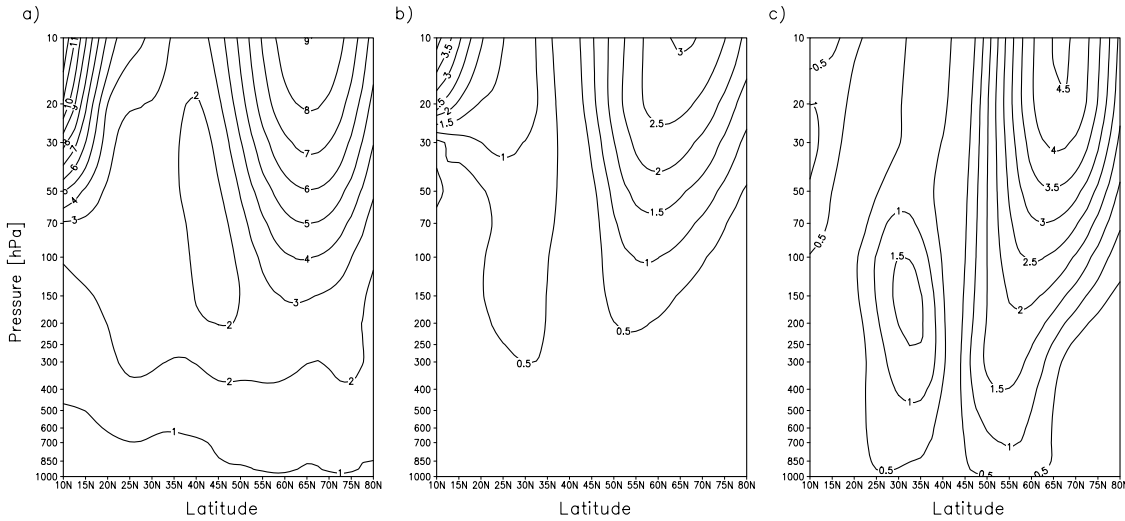

Figure 10. (a) Standard deviation of NH winter $\bar{u}$ for the period 1959–1998. (b) Standard deviation of NH winter $\bar{u}$ that is linearly related to the SIO index. (c) The same as (b), but for the TIO index. Contour intervals are 1 ms^{-1} in (a) and 0.5 ms^{-1} in (b) and (c).

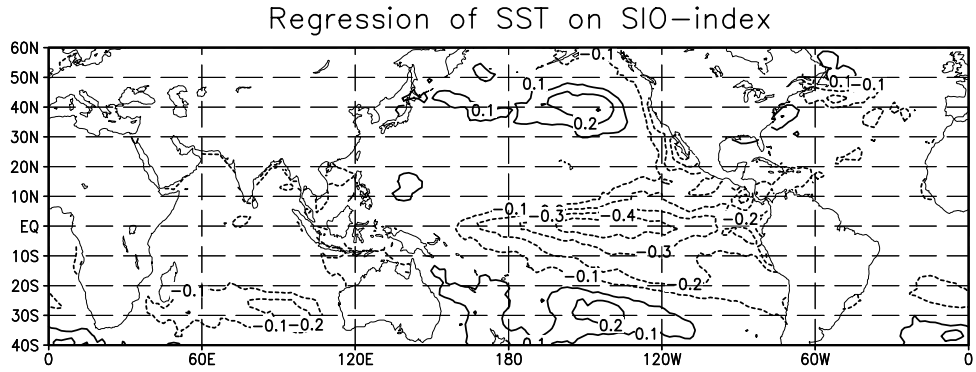

Figure 11. The same as in Figure 6, but on the normalized SIO index.

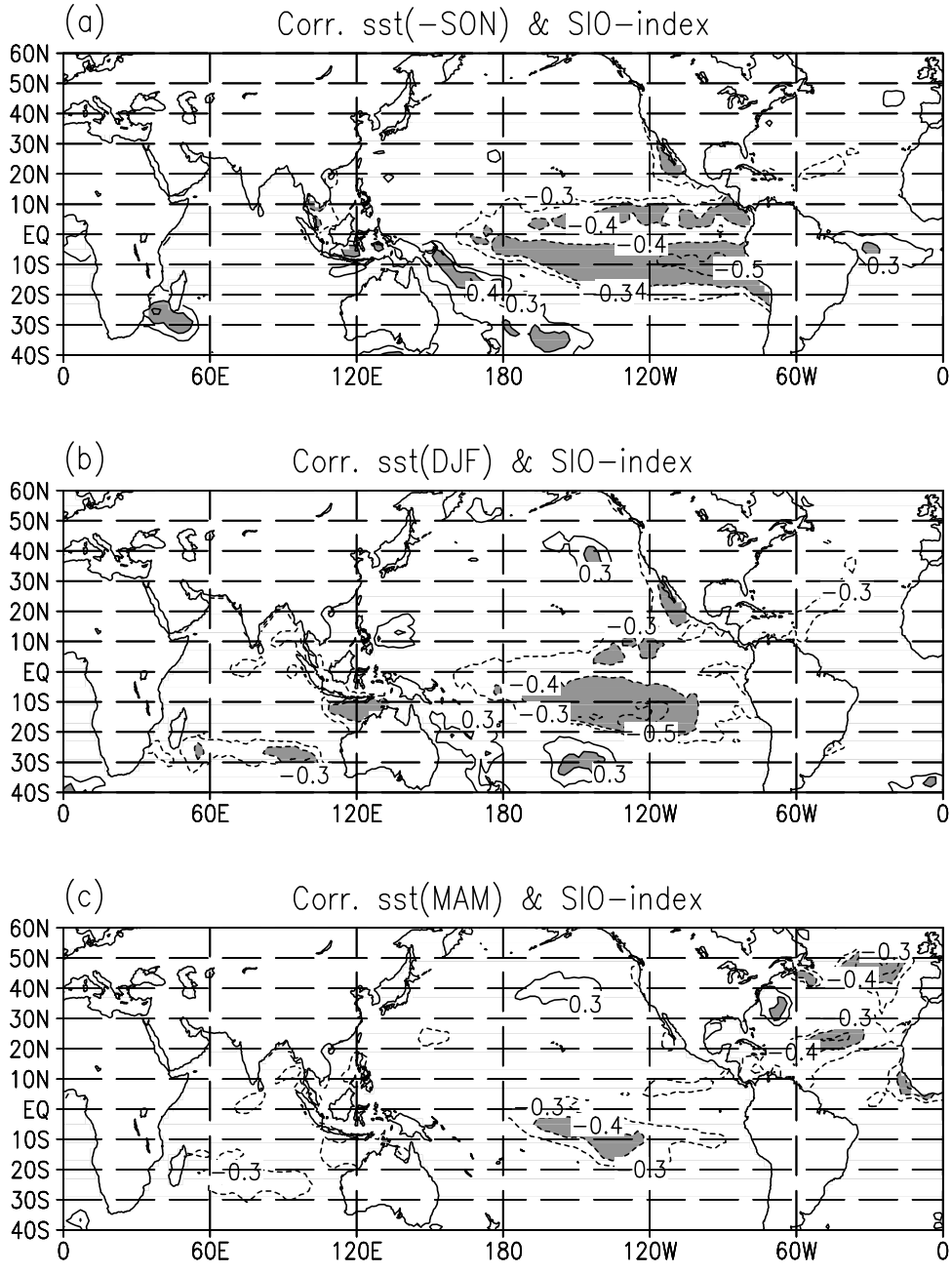

Figure 12. The same as in Figure 7, but for the SIO index.

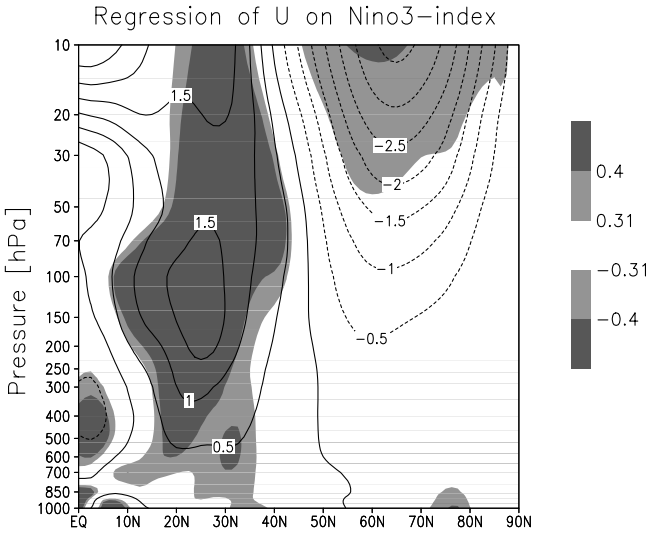

Figure 13. The same as in Figure 5a, but on the normalized Niño3 index. Contour interval is 0.5 ms^{-1}.

exists, but is only weak during the time interval of our data (1958–1998).

[24] We also calculated the lag correlation between the SST and time series of the SIO with a leading or lagging ocean as a check of the possible oceanic influence on the atmosphere or vice versa. Figure 12a presents the correlation coefficients between the SIO index and the preceding autumn (SON) SST anomalies. It is interesting to note that the correlations over equatorial Pacific are even stronger than during winter (DJF). On the contrary, in the following spring (MAM), the correlations over the tropical Pacific become weaker (Figure 12c). In fact, the significant correlations over the central and eastern tropical Pacific in Figure 12b can be traced back to the preceding spring, i.e., for a time lag of three seasons. This can be clearly seen from the lag-correlations between the SIO index and the average SST anomalies in Niño3 region (Figure 14). The SST anomalies are smoothed by three-month running means in order to deduce the relationships for seasonal means. We may also define a SST index by averaging the SST anomalies over the region 5°S–15°S and 150°W–110°W, which is located in the center of maximum correlations based on Figure 12b. The results of these lag-correlations are very similar with those for Niño3 index as shown in Figure 14. The only differences are the slightly higher correlations in the simultaneous winter and the preceding autumn and a somewhat smaller correlation in the preceding spring for this defined SST index. However, all correlations starting from the preceding spring to the simultaneous winter exceed the 95% significance level. The maximum negative correlation for Niño3 index is r = 0.55 in the three months (AMJ) with May as center month before the DJF SIO season. Even after examination on each individual month with the EDOF as *Davis* [1976], we can still draw the same conclusion as above. Therefore, the SIO is strongly influenced by ENSO. Our results are consistent with those of *Baldwin and O'Sullivan* [1995], who also found that ENSO's effect on the stratosphere via the modulation of the tropospheric flow was minor. We think that tropical SST might be directly coupled to the stratospheric atmosphere via the Brewer-Dobson circulation.

6. Discussions and Summary

[25] We have shown that the above-mentioned results are robust for seasonal means (DJF), and seasonal means are appropriate for the study of interannual variations. Based on monthly mean data (DJF) from 1958/1959 to 1997/1998, we found that the teleconnection patterns are reproducible and robust too. If we average over Dec-Feb to get the seasonal mean EP flux divergence, the results will be nearly the same as those in *Chen et al.* [2002] which were calculated directly from the seasonal mean data.

[26] In the paper, two teleconnection patterns in the EP flux divergence field due to planetary waves through WNs 1 to 3 in the NH winter troposphere and stratosphere are analyzed. Both patterns appear as dipole structures with divergence of EP flux in the north and convergence in the south, or vice versa. Their temporal evolutions measured by indices are different from each other, suggesting different dynamics of the teleconnection patterns. The tropospheric and stratospheric dipoles of EP flux divergence evolve on the interannual timescale and were referred to as the tropospheric interannual oscillation (TIO) and the stratospheric interannual oscillation (SIO), respectively. The planetary waves tend to be bent equatorward in the troposphere and lower stratosphere during a positive TIO phase. The upward and poleward refraction of planetary waves into the polar waveguide across the tropopause is shown to be closely linked to the meridional propagation of planetary waves in the troposphere. During the positive TIO phase, the upward and poleward propagation of planetary waves into the polar waveguide tends to be reduced. Examinations of individual zonal waves indicate that the tropospheric dipole of EP flux divergence comes basically from WN 3. The reduced refraction of planetary waves into the polar waveguide associated with positive TIO index is dominantly contributed from both WNs 1 and 2. On the other hand, the planetary waves tend to be bent equatorward in the

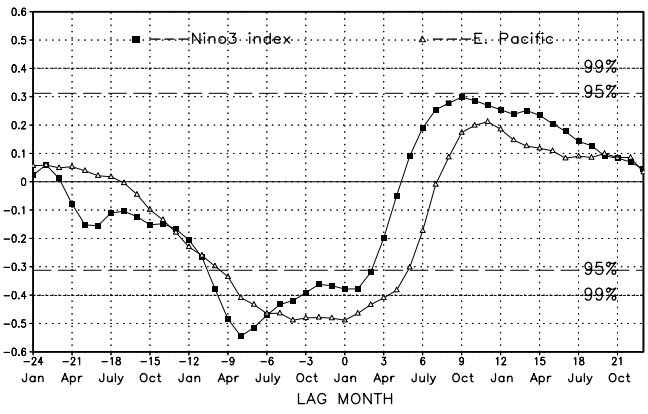

Figure 14. Lag-correlations between the SIO index and the SST anomalies in Niño3 region (5°N–5°S, 150°W–90°W) and in the tropical eastern Pacific (5°S–15°S and 150°W–110°W). The data are detrended by subtraction of local linear trends and smoothed by three-month running means.

midstratosphere during a positive SIO phase. These anomalous meridional wave propagations in the midstratosphere are shown to be independent of the tropospheric wave activity. Examinations of individual zonal waves indicate that the stratospheric dipole of EP flux divergence comes totally from WNs 1 and 2.

[27] With respect to the TIO, the regressed $\bar{u}$ pattern is an equivalent barotropic dipole extending from the lower troposphere to the upper stratosphere with weakened westerlies around 35°N, and enhanced westerlies around 55°N. The regressed 500 hPa geopotential height field is a predominantly zonally symmetric north-south fluctuation between the Arctic and the midlatitudes. Both patterns for $\bar{u}$ and geopotential height resemble the $\bar{u}$ and 500 hPa geopotential height regressed on the first EOF of the NH monthly mean SLP (the NAM index), respectively. The correlation between winter mean (DJF) NAM and TIO indices from 1958 to 1998 is significant at 99% level. Moreover, the regressed SST upon the TIO index exhibits a sandwich pattern in the North Pacific and a tripole pattern in the North Atlantic. The significant correlations will not appear when the SST leads the TIO for one season, but will persist to the following season especially in the North Atlantic. This indicates forcing of the ocean by the atmosphere. Therefore, our results suggest that the TIO is closely related to the NAM and the planetary waves play an important role in the zonal-mean zonal wind anomalies associated with the NAM, which are consistent with previous studies. However, planetary wave fluxes are not the whole story. Recent work of *Lorenz and Hartmann* [2003] has also suggested that the synoptic eddies contribute more to the annular mode related variability at tropospheric levels in the NH winter than the quasi-stationary eddies. These are beyond the scope of the paper and it would be interesting to compare the contributions between the planetary waves and the transient baroclinic waves in a future study.

[28] For the SIO, the regression map of $\bar{u}$ is a north-south dipole in the midstratosphere. However, the spatial structure of the regressed 500 hPa geopotential height on the SIO index is an augmented PNA wave train, which closely resembles the 500 hPa geopotential height regressed on the second EOF of the NH monthly mean SLP. Both the correlations of the SIO index to anomalous $\bar{u}$ and 500 hPa geopotential height are only moderate. Moreover, our results suggest that the leading EOF of stratospheric $\bar{u}$ variability reflects mainly the variations in the total amount of wave activity entering the stratosphere, which is closely associated with the TIO. With the teleconnectivity one can find a stratospheric variation of anomalous north-south planetary wave propagation, which is independent of the total amount of wave activity entering the stratosphere. The anomalous wave propagation may induce dynamical transport of trace gas, such as ozone, and exert an influence on their distribution. Our study may help to understand the climate change in the stratosphere.

[29] Further correlation analysis indicates that the SIO is in close association with the SST anomalies over the central and eastern tropical Pacific, which indicates basically an ENSO pattern. In addition, the significant correlations between the SIO index and the tropical eastern Pacific SST anomaly can be traced back to the preceding spring, which suggests a strong impact of ENSO on the SIO. Planetary waves tend to be bent poleward in the midstratosphere during a warm event. The situation tends to be reverse for a cold event. The mechanism for this connection between SST and the midstratospheric planetary wave activity needs to be studied further.

[30] **Acknowledgments.** We would like to thank three anonymous reviewers for their helpful comments and suggestions. The first author would like to thank Prof. Ronghui Huang and Dr. S. K. Dhaka for useful discussions. He is also very grateful to Koichiro Tsuji, Yoshio Kawatani, Kengo Sudo, Kei Sakamoto and Miho Yamamori for their help throughout this work in CCSR. This work is supported by NSFC under grant 40231005 and CAS under grants KZ CX3-SW-218, ZKCX2-SW-210 and G1998040900.

References

Ambaum, M. H. P., B. J. Hoskins, and D. B. Stephenson, Arctic Oscillation or North Atlantic Oscillation?, *J. Clim.*, *14*, 3495–3507, 2001.

Andrews, D. G., J. R. Holton, and C. B. Leovy, *Middle Atmosphere Dynamics*, 489 pp., Academic, San Diego, Calif., 1987.

Baldwin, M. P., and T. J. Dunkerton, Propagation of the Arctic Oscillation from the stratosphere to the troposphere, *J. Geophys. Res.*, *104*, 30,937–30,946, 1999.

Baldwin, M. P., and D. O'Sullivan, Stratospheric effects of ENSO-related tropospheric circulation anomalies, *J. Clim.*, *8*, 649–667, 1995.

Baldwin, M. P., X. Cheng, and T. J. Dunkerton, Observed correlations between winter-mean tropospheric and stratospheric circulation anomalies, *Geophys. Res. Lett.*, *21*, 1141–1144, 1994.

Branstator, G., The relationship between zonal mean flow and quasi-stationary waves in the midtroposphere, *J. Atmos. Sci.*, *41*, 2163–2178, 1984.

Chen, W., and R.-H. Huang, The modulation of planetary wave propagation by the tropical QBO zonal winds and the associated effects in the residual meridional circulation, *Contrib. Atmos. Phys.*, *72*, 187–204, 1999.

Chen, W., H.-F. Graf, and M. Takahashi, Observed interannual oscillations of planetary wave forcing in the Northern Hemisphere winter, *Geophys. Res. Lett.*, *29*(22), 2073, doi:10.1029/2002GL016062, 2002.

Czaja, A., and C. Frankignoul, Observed impact of Atlantic SST anomalies on the North Atlantic Oscillation, *J. Clim.*, *15*, 606–623, 2002.

Davis, R. E., Predictability of sea surface temperature and sea level pressure anomalies over the North Pacific Ocean, *J. Phys. Oceanogr.*, *6*, 249–266, 1976.

Deser, C., On the teleconnectivity of the "Arctic Oscillation,"*Geophys. Res. Lett.*, *27*, 779–782, 2000.

DeWeaver, E., and S. Nigam, Do stationary waves drive the zonal-mean jet anomalies of the Northern Winter?, *J. Clim.*, *13*, 2160–2176, 2000.

Dunkerton, T. J., and M. Baldwin, Quasi-biennial modulation of planetary-wave fluxes in the Northern Hemisphere winter, *J. Atmos. Sci.*, *48*, 1043–1061, 1991.

Edmon, H. J., Jr., B. J. Hoskins, and M. E. McIntyre, Eliassen-Palm cross sections for the troposphere, *J. Atmos. Sci.*, *37*, 2600–2616, 1980.

Frankignoul, C., and K. Hasselmann, Stochastic climate models. Part II: Application to sea-surface temperature variability and thermocline variability, *Tellus*, *29*, 289–305, 1977.

Fusco, A. C., and M. L. Salby, Interannual variations of total ozone and their relationship to variations of planetary wave activity, *J. Clim.*, *12*, 1619–1629, 1999.

Graf, H.-F., I. Kirchner, and J. Perlwitz, Changing lower stratospheric circulation: The role of ozone and green-house gases, *J. Geophys. Res.*, *103*, 11,251–11,261, 1998.

Hamilton, K., An examination of observed Southern Oscillation effects in the Northern Hemisphere stratosphere, *J. Atmos. Sci.*, *50*, 3468–3473, 1993.

Hoerling, M. P., J. W. Hurrell, and T. Xu, Tropical origins for recent North Atlantic climate change, *Science*, *292*, 90–92, 2001.

Holton, J. R., and H.-C. Tan, The quasi-biennial oscillation in the northern hemisphere lower stratosphere, *J. Meteorol. Soc. Jpn.*, *60*, 140–147, 1982.

Kalnay, E., et al., The NCEP/NCAR 40-Year Reanalysis Project, *Bull. Am. Meteorol. Soc.*, *77*, 437–471, 1996.

Kinnersley, J. S., Interannual variability of stratospheric zonal wind forced by the northern lower-stratospheric large-scale waves, *J. Atmos. Sci.*, *55*, 2270–2283, 1998.

Kistler, R., et al., The NCEP-NCAR 50-year reanalysis: Monthly means CD-ROM and documentation, *Bull. Am. Meteorol. Soc.*, *82*, 247–267, 2001.

Kodera, K., On the origin and nature of the interannual variability of the winter stratospheric circulation in the Northern Hemisphere, *J. Geophys. Res.*, *100*, 14,077–14,087, 1995.

Kodera, K., and H. Koide, Spatial and seasonal characteristics of recent decadal trends in the northern hemispheric troposphere and stratosphere, *J. Geophys. Res.*, *102*, 19,433–19,447, 1997.

Kuroda, Y., and K. Kodera, Role of planetary waves in the stratosphere-troposphere coupled variability in the Northern Hemisphere winter, *Geophys. Res. Lett.*, *26*, 2375–2378, 1999.

Labitzke, K., On the interannual variability of the middle stratosphere during the northern winters, *J. Meteorol. Soc. Jpn.*, *60*, 124–139, 1982.

Latif, M., K. Arpe, and E. Roeckner, Oceanic control of decadal North Atlantic sea level pressure variability in winter, *Geophys. Res. Lett.*, *27*, 727–730, 2000.

Limpasuvan, V., and D. L. Hartmann, Eddies and the annular modes of climate variability, *Geophys. Res. Lett.*, *26*, 3133–3136, 1999.

Limpasuvan, V., and D. L. Hartmann, Wave-maintained annular modes of climate variability, *J. Clim.*, *13*, 4414–4429, 2000.

Lorenz, D. J., and D. L. Hartmann, Eddy-zonal flow feedback in the Northern Hemisphere winter, *J. Clim.*, *16*, 1212–1227, 2003.

Marshall, J., et al., North Atlantic climate variability: Phenomena, impacts and mechanisms, *Int. J. Climatol.*, *21*, 1863–1898, 2001.

Matsuno, T., Vertical propagation of stationary planetary waves in the winter Northern Hemisphere, *J. Atmos. Sci.*, *27*, 871–883, 1970.

Niwano, M., and M. Takahashi, The influence of the equatorial QBO on the Northern Hemisphere winter circulation of a GCM, *J. Meteorol. Soc. Jpn.*, *76*, 453–461, 1998.

Pawson, S., and M. Fiorino, A comparison of reanalyses in the tropical stratosphere. Part 3: Inclusion of the pre-satellite data era, *Clim. Dyn.*, *15*, 241–250, 1999.

Perlwitz, J., and H.-F. Graf, The statistical connection between tropospheric and stratospheric circulation of the Northern Hemisphere in winter, *J. Clim.*, *8*, 2281–2295, 1995.

Randel, W. R., A study of planetary waves in the southern winter troposphere and stratosphere. Part I: Wave structure and vertical propagation, *J. Atmos. Sci.*, *44*, 917–935, 1987.

Reynolds, R., and T. M. Smith, A high-resolution global sea surface temperature climatology, *J. Clim.*, *6*, 1571–1583, 1995.

Rind, D., D. T. Shindell, P. Lonergan, and N. K. Balachandran, Climate change of the middle atmosphere. Part III: The doubled CO_2 climate revisited, *J. Clim.*, *11*, 876–894, 1998.

Robinson, W. A., The application of the quasi-geostrophic Eliassen-Palm flux to the analysis of stratospheric data, *J. Atmos. Sci.*, *43*, 1017–1023, 1986.

Robinson, W. A., Review of WETS—The workshop on extratropical SST anomalies, *Bull. Am. Meteorol. Soc.*, *81*, 567–577, 2000.

Rodwell, M. J., D. P. Rowell, and K. C. Folland, Oceanic forcing of the wintertime North Atlantic Oscillation and European climate, *Nature*, *398*, 320–323, 1999.

Salby, M., P. Callaghan, P. Keckhut, S. Godin, and M. Guirlet, Interannual changes of temperature and ozone, *SPARC Newsl.*, *15*, 2000.

Scinocca, J. F., and P. H. Haynes, Dynamical forcing of stratospheric planetary waves by tropospheric baroclinic eddies, *J. Atmos. Sci.*, *55*, 2361–2392, 1998.

Shindell, D. T., D. Rind, and P. Lonergan, Increased polar stratospheric ozone losses and delayed eventual recovery due to increasing greenhouse gas concentrations, *Nature*, *392*, 589–592, 1998.

Shindell, D. T., R. L. Miller, G. A. Schmidt, and L. Pandolfo, Simulation of recent northern winter climate trends by greenhouse gas forcing, *Nature*, *399*, 452–455, 1999.

Thompson, D. W. J., and J. M. Wallace, The Arctic Oscillation signature in the wintertime geopotential height and temperature fields, *Geophys. Res. Lett.*, *25*, 1297–1300, 1998.

Thompson, D. W. J., and J. M. Wallace, Annual modes in the extratropical circulation. Part I: Month-to-month variability, *J. Clim.*, *13*, 1000–1016, 2000.

Thompson, D. W. J., J. M. Wallace, and G. C. Hegerl, Annual modes in the extratropical circulation, Part II: Trends, *J. Clim.*, *13*, 1018–1036, 2000.

Ting, M., M. P. Hoerling, T. Xu, and A. Kumar, Northern Hemisphere teleconnection patterns during extreme phases of the zonal-mean circulation, *J. Clim.*, *9*, 2615–2633, 1996.

Wallace, J. M., and D. S. Gutzler, Teleconnections in the geopotential height field during the northern hemisphere winter, *Mon. Weather Rev.*, *109*, 784–812, 1981.

Wallace, J. M., and D. W. J. Thompson, The Pacific center of action of the Northern Hemisphere Annular Mode: Real or artifact?, *J. Clim.*, *15*, 1987–1991, 2002.

Watanabe, M., and M. Kimoto, Ocean atmosphere thermal coupling in the North Atlantic: A positive feedback, *Q. J. R. Meteorol. Soc.*, *126*, 3343–3369, 2000.

Yamazaki, K., and Y. Shinya, Analysis of the Arctic Oscillation simulated by AGCM, *J. Meteorol. Soc. Jpn.*, *77*, 1287–1298, 1999.

W. Chen, Laboratory of Numerical Modeling for Atmospheric Sciences and Geophysical Fluid Dynamics (LASG), Institute of Atmospheric Physics, Chinese Academy of Sciences, 100080 Beijing, China. (chenw@lasg.iap.ac.cn)

H.-F. Graf, Max-Planck-Institute for Meteorology, D-20146 Hamburg, Germany.

M. Takahashi, Center for Climate System Research, University of Tokyo, 153 Tokyo, Japan.